IEA Wind Task 46

Erosion of wind turbine blades

Model to predict annual energy production loss based on blade erosion class

Technical report

David Maniaci

Alexander Meyer Forsting

Athanasios Barlas

Christian Bak

Anders Smærup Olsen

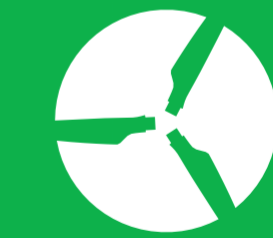

iea win

Technical Report

Model to predict annual energy production loss based on blade erosion class

Prepared for the
International Energy Agency Wind Implementing Agreement

Prepared by

David Maniaci – Sandia National Laboratories
Alexander Meyer Forsting – DTU Wind and Energy Systems
Athanasios Barlas – DTU Wind and Energy Systems
Christian Bak – DTU Wind and Energy Systems
Anders Smærup Olsen – DTU Wind and Energy Systems

Date February 2025

Sandia National Laboratories is a multimission laboratory managed and operated by National Technology and Engineering Solutions of Sandia, LLC, a wholly owned subsidiary of Honeywell International Inc., for the U.S. Department of Energy's National Nuclear Security Administration under contract DE-NA0003525.
SAND2025-02634R

Purpose

Leading edge erosion (LEE) of wind turbine blades has been identified as a major factor in decreased wind turbine blade lifetimes and energy output over time. Accordingly, the International Energy Agency Wind Technology Collaboration Programme (IEA Wind TCP) has created the Task 46 to undertake cooperative research in the key topic of blade erosion. Participants in the task are given in Table 1.

The Task 46 under IEA Wind TCP is designed to improve understanding of the drivers of LEE, the geospatial and temporal variability in erosive events; the impact of LEE on the performance of wind plants and the cost/benefit of proposed mitigation strategies. Furthermore Task 46 seeks to increase the knowledge about erosion mechanics and the material properties at different scales, which drive the observable erosion resistance. Finally, the Task aims to identify the laboratory test setups which reproduce faithfully the failure modes observed in the field in the different protective solutions.

This report is a product of Work Package 3: Wind Turbine Operation with Erosion**.**

The objectives of the work summarized in this report are to:

- Develop a common model of performance loss due to leading edge roughness and erosion standardized classes.

Table 1: IEA Wind Task 46 Participants.

Country	Contracting Party	Active Organizations
Belgium	The Federal Public Service of Economy, SMEs, Self-Employed and Energy	Engie
Canada	Natural Resources Canada	WEICan
Denmark	Danish Energy Agency	DTU (OA), Hempel, Ørsted A/S, PowerCurve, Siemens Gamesa Renewable Energy
Finland	Business Finland	VTT
Germany	Federal Ministry for Economic Affairs and Energy	Fraunhofer IWES, Covestro, Emil Frei (Freilacke), Nordex Energy SE, RWE, DNV, Mankiewicz, Henkel
Ireland	Sustainable Energy Authority of Ireland	South East Technology University, University of Galway, University of Limerick
Japan	New Energy and Industrial Technology Development Organization	AIST, Asahi Rubber Inc., Osaka University, Tokyo Gas Co.
Netherlands	Netherlands Enterprise Agency	TU Delft, TNO
Norway	Norwegian Water Resources and Energy Directorate	Equinor, University of Bergen, Statkraft
Spain	CIEMAT	CENER, Aerox, CEU Cardenal Herrera University, Nordex Energy Spain
United Kingdom	Offshore Renewable Energy Catapult	ORE Catapult, University of Bristol, Lancaster University, Imperial College London, Ilosta, Vestas
United States	U. S. Department of Energy	Cornell University, Sandia National Laboratories, 3M

Table of Contents

Purpose 3
1. Introduction 9
2. Aerodynamic Performance Categorization 9
3. Spanwise Distribution of Aerodynamic Loss Categories 11
4. AEP Erosion Loss Model General Description 16
4.1 AEP Erosion Loss Model Components 16
4.2 Sandia Model Description and Results 17
4.3 DTU Erosion Loss Modeling of the IEA 15 and 22 MW 24
5. Future Work 35
6. Conclusions 36
References 37

List of Figures

Figure 1: Power loss defined in Region 2 of the power curve. 10
Figure 2: Comparison of damage distributions. 13
Figure 3: Distribution of ‘damage type’ structural and aerodynamic severity levels. 13
Figure 4: Spanwise distribution of aerodynamic damage categories 14
Figure 5: Likelihood of damage appearing across all blades of a turbine 15
Figure 6: Radial damage distribution 15
Figure 7: Spanwise damage model for the erosion category 17
Figure 8: Stair-step simplified spanwise damage model 18
Figure 9: Impact of exponent in erosion damage model. 18
Figure 10: Field measurements and wind tunnel test of Cat 4 erosion 19
Figure 11: Lift and drag change with erosion on the NACA 63_3-418 airfoil 20
Figure 12: Airfoil polar with erosion correction: FFA-W3-211. 21
Figure 13: Airfoil polar with erosion correction: FFA-W3-241. 21
Figure 14: Power curve with erosion of IEA 22 MW wind turbine. 22
Figure 15: Power loss versus wind speed for range of erosion cases. 22
Figure 16: Region 2 power loss for range of erosion cases. 23
Figure 17: AEP loss for range of erosion cases, 8.5 m/s mean wind speed 24
Figure 18: Dimensions of the IEA 15 MW and 22 MW offshore turbines 25
Figure 19: Thickness distributions of the IEA 15 and 22 MW offshore turbines 25
Figure 20: CFD resolved erosion type LE damage on the FFA-W3-241 26
Figure 21: Performance of the FFA-W3-211 and FFA-W3-241. 27
Figure 22: Change in aerodynamic performance with respect to mixed polars. 27
Figure 23: Mean power curves for the IEA 15 MW and IEA 22 MW 29
Figure 24: Change in mean power and its variability. 29
Figure 25: Change in rotor speed and pitch 30
Figure 26: Angle-of-attack and lift coefficient variation at 90% of radius. 31
Figure 27: Changes in radial angle-of-attack and lift coefficient distributions. 32
Figure 28: Radial lift-to-drag ratio distributions. 33
Figure 29: Comparison of power loss predictions by HAWC2 and SALT 34
Figure 30: Tip speed ratio curves from different models. 34

List of Tables

Table 1: IEA Wind Task 46 Participants. 4
Table 2: AEP loss due to erosion. 11
Table 3: SALT turbine inputs 32
Table 4: Predictions of AEP changes 35

Executive Summary

This report summarizes the state of the art in methods used to model the annual energy production (AEP) loss caused by the leading edge erosion of wind turbine blades. A summary of the relationship between blade damage categorization and aerodynamic performance categorization is presented. The definition of spanwise erosion damage distribution is very important to accurately predicting the effect of erosion on AEP loss, with methods presented that utilize actual field observations as well as models of the relative distribution of damage.

To determine the spanwise distribution of aerodynamically relevant damages over wind turbine blades, image-based maintenance reports from a Northern European offshore wind farm were analyzed. Overall, the analysis re-confirms that the spanwise aerodynamic damage severity strongly depends on the distance from the tip; however, it also highlights that small, but aerodynamically relevant, damages are less likely to be identified and that the damage progression is highly stochastic. This study shows that the spanwise extent of the damages should be considered when assessing the radial distribution of the damages over the blade. Future work includes developing an idealized radial severity distribution that accounts for the uncertainty in the aerodynamic categorization.

The current state of the art in predicting AEP loss is to use either calibrated computational models of the effect of erosion on airfoil force data or to use high quality wind tunnel measurements of such effects, both methods are utilized in this report. The IEA15 MW and IEA 22 MW reference wind turbines were selected as modern erosion reference models and two approaches are presented to simulate the impact of erosion on its power and AEP production. The results show different trends than past work, in part attributed to the active pitching of the IEA 22 MW turbine controller in region 2 operation. The effect of turbulence and sheared inflow on relative loss in AEP was minimal and the IEA 15 MW and 22 MW show distinctly different responses to erosion, as they are operated differently below rated wind speed. This work will continue in phase 2 of IEA Wind Task 46, targeting standardization of many of the required modeling methods for AEP loss prediction, continued benchmarking of the models, and exploration of the effects on a range of turbine models and site conditions.

1. Introduction

The roughness and surface damage caused by erosion reduces the aerodynamic performance of wind turbine blades, reducing energy output from turbines. This report captures methods used to model the annual energy production (AEP) loss due to leading edge erosion. The relationship between blade erosion categories and AEP loss is of practical interest to those relying on the power production of wind turbines to be able assess the cost tradeoff of repairs, leading edge protection (LEP), and AEP loss. The current state of the art in predicting AEP loss is to use either calibrated computational models of the effect of erosion on airfoil force data or to use high quality wind tunnel measurements of such effects, both methods are utilized in this report. The IEA 22 MW reference wind turbine was selected as a modern common erosion reference model and two approaches are presented to simulate the impact of erosion on its power and AEP production.

2. Aerodynamic Performance Categorization

A step toward erosion classification standardization was taken in the Leading Edge Erosion Classification System report (Maniaci, et al., 2022). The report described existing systems for erosion classification and brought them together into a common framework. The system defines discrete severity levels of erosion and maps them to four classification categories:

- Visual Condition (concerning blades with/without leading edge protection)
- Mass Loss
- Aerodynamic Performance
- Structural Integrity

Erosion is typically classified based on the visual observation; however, the impact of the erosion on physical quantities is what is of most concern to a wind farm owner (structural integrity, repair time, and AEP loss). The common erosion classification system creates a map between these categories. The present report on AEP loss directly relates to the Aerodynamic Performance categorization.

Aerodynamic performance categorization is most concerned with the impact of erosion and leading edge protection on wind turbine power and AEP due to the associated decrease in aerodynamic performance of the wind turbine blades. Such decreased performance is the result of increased roughness due to erosion and due to damaged leading edge protection; however, even some types of undamaged leading edge protection will cause decreased performance relative to an ideal, clean blade.

The effect of leading edge erosion on wind turbine AEP is found by integrating the power loss across the entire operating wind speed range; with several example investigations available (Maniaci, et al., 2020; Bak, et al., 2020). The erosion categories in the classification system are related to the power loss in normal Region 2 operation for a variable speed, variable pitch horizontal axis wind turbine, when the turbine is operating at or near the design tip speed ratio, typically 6-8 m/s, as illustrated in Figure 1.

Typically, a severity rating is given for an entire rotor, although there can be variation from blade to blade, and there is always variation across the blade span. The spanwise extent of erosion and blade to blade variations must be included in assessing the power loss for a turbine. In order to account for changes in the erosion category of a blade as the local conditions vary, the following rule has been used: *When 5% of blade span is in a given class the blade is considered that class or if a higher class changes the response, the blade class is increased*. The blade spanwise location used to define the overall blade class is not standardized and this selection has a non-negligible impact on performance loss, as explored in Sections 3 and 4 of this report.

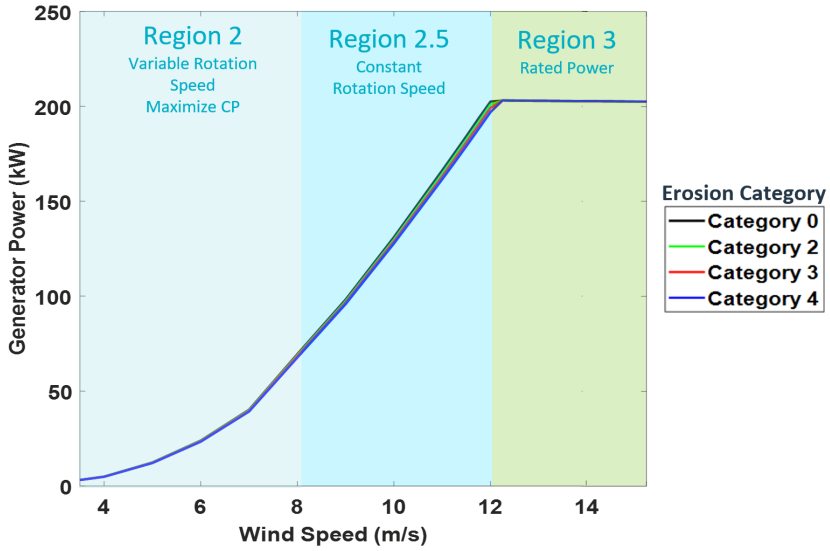

Figure 1. Power loss is defined in Region 2 of the power curve.

In addition to the effect on power loss, the aerodynamic performance categories are also defined by the changes in the blade boundary layer conditions due to changes in the equivalent roughness that are caused by leading edge erosion or damage to the LEP. These categories are summarized below and described in more detail in the associated erosion classification report (Maniaci, et al., 2022). Region 2 power loss from the erosion severity categories can be mapped to the annual energy production (AEP) loss.

Category 0: Flow not disturbed. Roughness effects are damped by the viscosity of the flow.

Category 1: Region 2 Power loss <1%. The transition point is moved forward toward the leading edge.

Category 2: Region 2 Power loss 1%, Moderate loss to L/D and CL_max, (-20% and -5%). The transition point is moved forward to the leading edge.

Category 3: Noticeable loss to L/D and CL_max (-30% and -5-10%). The flow is fully turbulent downstream of the roughness elements in eroded regions of the blade span.

Category 4: Significant loss to L/D (> -40%) and CL_max (> -10%). The flow separates in downstream locations due to the boundary layer weaknesses against adverse pressure gradients given by airfoil geometry.

Category 5: Severe loss to L/D and CL_max due to flow separation and a lack of laminar flow.

The AEP loss of a wind turbine depends heavily on the mean wind speed of a site as well as the erosion damage distribution along the blades, as shown in Table 2. The results in this table are for a relatively high specific power pitch regulated, variable speed wind turbine using a Rayleigh wind distribution and did not include the category 1 and 5 cases. The 'Erosion Category' is the blade erosion category defined by the erosion category at 95% span with the blade category damage distribution being proportional to the incoming velocity to an exponent of 6.7 (Maniaci, et al., 2020). The design of a turbine, its controller, and site specific characteristics will all change the AEP loss to blade erosion category mapping.

Table 2: AEP loss due to erosion. Relative to no erosion for a range of mean wind speeds using a Rayleigh wind distribution. Based on power curve cloud results from Ref. (Maniaci, et al., 2020). Note categories 1 and 5 were not modeled in the study.

Erosion Category	Mean Wind Speed (m/s)				
	4	6	7.5	8.5	10
0	0.0%	0.0%	0.0%	0.0%	0.0%
2	-1.0%	-0.9%	-0.7%	-0.6%	-0.4%
3	-1.9%	-1.6%	-1.3%	-1.1%	-0.8%
4	-3.0%	-2.6%	-2.2%	-1.9%	-1.6%

Turbines with simpler controllers and relatively higher specific power will likely see a similar AEP loss mapping to the table above and should be able to be modeled using more simple erosion loss models. Turbines with more advanced controllers, sensors, and with lower specific power designs will see a different mapping that requires physics based models to capture the power and AEP loss due to erosion. Two studies of more modern reference turbines with more advanced controllers and larger rotors will be explored in the following sections.

3. Spanwise Distribution of Aerodynamic Loss Categories

Offshore Wind Farm Inspection Data

To determine the spanwise distribution of aerodynamically relevant damages over wind turbine blades, image-based maintenance reports from a Northern European wind farm were analyzed. The farm comprises a single turbine model and none of the blades had leading edge protection at the time. The inspections were performed over three years, but there is only a single report per turbine. The blades were inspected from all sides (leading edge (LE), trailing edge (TE), suction side (SS) and pressure side (PS)) using a ground-based camera. The images were annotated manually by the inspection company by drawing boxes around findings and labeling them regarding their type (Lighting strike, erosion, LPS ...), blade chordwise position (LE, TE, ...) and material damage layer (paint, laminate …). Furthermore, the spanwise extend and position from the root were added and a unique ID attached to them. Depending on type, size and damage layer the findings were categorized into five severity levels:

1. Minor non-structural with no influence on structure or performance
2. Minor structural with potential performance impact. No risk of fast progression.
3. Minor structural with performance impact. Risk of fast progression.
4. Structural defects requiring timely action
5. Major structural defects that requiring immediate action to avoid catastrophic failure

Note that the above are not the actual definitions but represent a shortened summary. Whilst the focus of this categorization lies on structural significance, at least the first three also indicate the level of expected performance loss.
In total data for 233 blades was made available containing 2905 labelled findings of which 63% were located on or around the leading edge. As size and spanwise location of the damages are needed to establish their spanwise distribution, 54% of the entries remained. This remaining set was collected over distinct, short periods with 3 years in-between, but not for the same turbines. One year contains 1067 entries whereas the other has 500. Unless specifically mentioned they are not treated independently.
Upon closer inspection of the images it became apparent that the original categories did not reflect aerodynamic performance loss and hence the findings were manually re-categorized into aerodynamic severity classes (Visbech, et al., 2024):

a. Factory clean
b. Few pits and gouges
c. Frequent pits and gouges
d. Eroded top coat
e. Onset of laminate exposure
f. Laminate exposure + sharp edges

Aerodynamic re-categorization
The categorization was performed by a single individual, however due to variations in contrast, image quality, lighting, there remains some level of uncertainty in applying the correct category to each finding. Figure 2 compares how the distribution of findings changes when applying the aerodynamic, instead of the original, structural severity classes. There is a clear shift towards higher severity levels (Figure 2, left) when applying the aerodynamic categorization scheme and the distribution of damages becomes uniform above level b (>1). Hence the dataset contains enough realizations within the different categories, except for the lowest, which hints at the difficulty of identifying small damages, like individual small-scale pits, from images. When comparing how damages are relabeled (Figure 2, right) only weak correlation is observed between the two classifications with a large number of damages of high aero severity falling into low structural classes. As all damages were also labelled by ‘damage type’, Figure 3 explores how their distribution across the different severity levels is affected by the respective scheme (left: structural, right: aero). Whilst the type labelling was to some extent found to be inconsistent and ill defined, the aero classification seems to shift types that are associated with higher aerodynamic losses (erosion) towards higher severity levels, as expected.

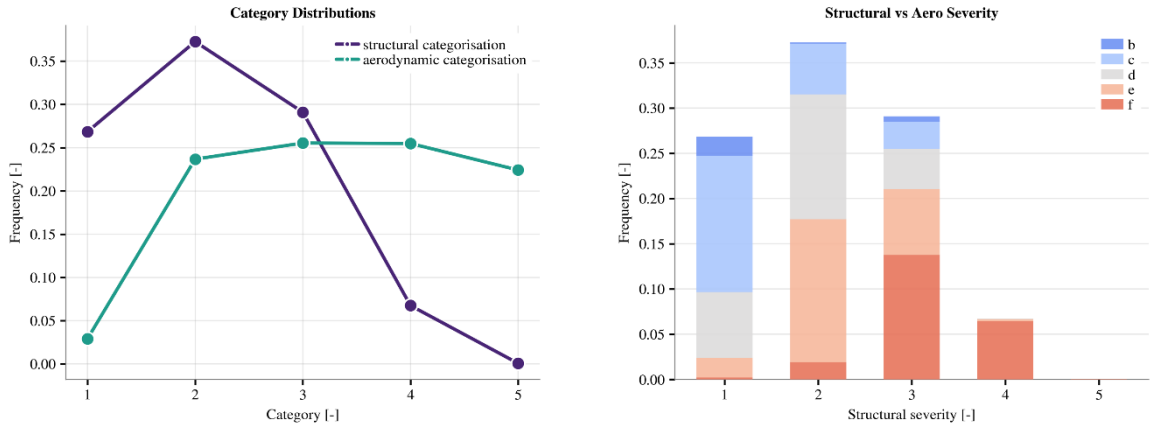

Figure 2: Comparison of damage distributions depending on categorization scheme. On the left 1='b', 2='c' … in the aerodynamic categorization.

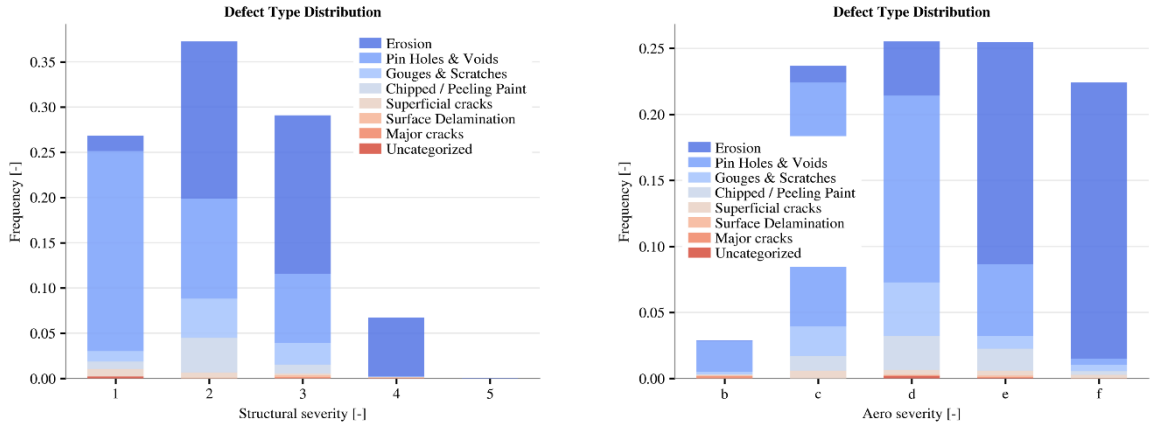

Figure 3: Distribution of 'damage type' label with structural and aerodynamic severity levels.

Spanwise Statistics

As the spanwise location (distance from blade root) and size of most damages was available, the distribution of aerodynamic severity levels along the blade span within the wind farm can be computed. This can be done by splitting the blade into spanwise sections and either counting the number of damages per section or the cumulative length of all damages within each section.

Here the blade is split into 20 uniform sections, i.e. 5% of span, and first the number of counts per section is computed. If the damage falls between sections, the count is added to each section that contains part of the damage. Whilst it is possible to have multiple damages of the same category falling within each section, the count per damage is limited to one. The number of damages per category falling within a section are subsequently summed and normalized by the total number of blades analyzed. The distribution is shown in the left of Figure 4, which also indicates that in the outer 25% of the blade it is likely to find multiple damages of varying severity. As expected, the number of damages increases towards the tip and they become more

severe. Damages of category greater ‘c’ only occur in the outer 40%. As all findings are of varying spanwise extent, simply counting the number of occurrences could be misleading, as it might give the impression that the entire section was covered by the damage. A more representative measure is to sum the total length of all damages of a certain category falling within each section (making sure to split damages that fall between sections) and normalize by the sum of all sections (cumulative sectional span in the wind farm). This gives a measure of the fraction of the total span in the wind farm that is damaged as function of span, which is presented on the right of Figure 4. This shows for instance that about 70% of the outer 10% of all blades in the farm have some form of damage, mostly of the highest severity. Comparing the two different measures of damage frequency, it is also clear that simply counting the frequency can be misleading, as for instance at 75% radius a damage will be found (normalized occurrence around 1), however it will not cover the entire section as indicated by the cumulative damage (about 0.24). It is only damages of category ‘e’ and ‘f’ that appear in the outer 10% of the blade that also cover larger parts of the blade sections, i.e. they are more spanwise homogenous. Splitting the dataset by year of collection has little effect on the spanwise distribution.

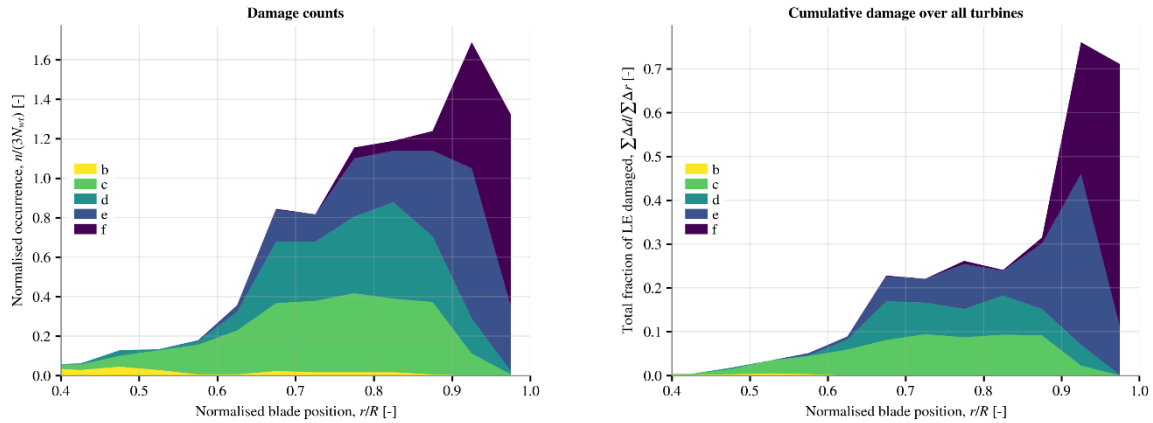

Figure 4: Spanwise distribution of aerodynamic damage categories; Left: Damages per section; Right: Cumulative length of damages.

Another measure of how deterministic the appearance of damages on blades are, is to determine whether finding a certain damage category on one section of a blade of a turbine implies that the other two should also have it. Afterall all blades are facing the same environmental conditions and run at the same speed, so they should accumulate the same fatigue damage. Figure 5 shows the likelihood that a damage of a certain severity is seen across all three blades by calculating the mean findings across all turbines per section if a damage was present. Whilst finding a damage of the lowest category on one blade of the turbine does not imply that the entire turbine is affected, finding level ‘f’ damage in the outer 5% of the blade certainly is. At 83% radius it is also interesting to see that the likelihood of all categories except ‘f’ are similar, showing that the appearance of this type of damage is highly stochastic or very quick to progress to higher severity levels.

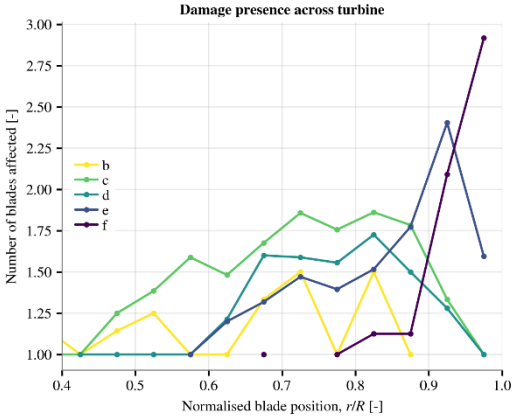

Figure 5: Likelihood of damage appearing across all blades of a turbine

Finally, the radial damage evolution can be estimated by investigating its relative evolution along the blade, which requires the categories to be weighted. In absence of alternatives and more detailed damage definitions, the weights attached to the categories are: b=1.0, c=2.0, …, f=5.0. Using the cumulative damage distributions from Figure 4 and normalizing with the weighted cumulative damage at the tip, the radial damage distribution can be computed as shown in Figure 6. Fitting a power law to data from r/R >=0.5, gives an exponent of 6.05, which indicates that the damage severity, as defined here, evolves with sectional speed to that power – similar to exponents reported in literature.

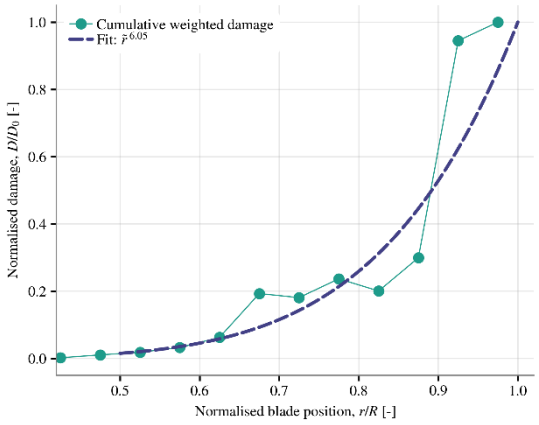

Figure 6: Radial damage distribution, estimated from the cumulative damage distribution, weighted by category.

Conclusion

Overall, the analysis of inspection data from a large offshore wind farm re-confirms that the spanwise aerodynamic damage severity strongly depends on the distance from the tip, as expected from material fatigue correlating with impact velocity. However, it also highlights that small, but aerodynamically relevant, damages are less likely to be identified (this might change with improving inspection techniques) and that the damage progression is highly stochastic, with blades on the same turbine suffering from very different damages, except if the highest severity level has been reached. Furthermore, this study shows that the spanwise extent of

the damages should be considered when assessing the radial distribution of the damages over the blade, as they usually only cover a small fraction of a blade section. This data could potentially be used in the future to develop an idealized radial severity distribution, however it needs to be kept in mind that the aerodynamic categorization of damages performed here remains highly uncertain and should be improved.

4. AEP Erosion Loss Model General Description

Power loss and the resulting AEP loss are very important to predict despite the lack of direct validation data, driving loss of revenue and regular repair costs. The current state of the art in predicting these values is to use either calibrated computational models of the effect of erosion on airfoil force data or to use high quality wind tunnel measurements of such effects. A spanwise damage model is used to distribute the airfoil polar data along the blade span. The spanwise eroded airfoil data is then used in simulations of the rotor to predict the power loss with erosion. Such predictions can include the interaction of the controller with simulated turbulent winds and the change of the controller response for pitch and speed regulation of the turbine with the effect of erosion on the airfoil lift and drag.

To validate the performance or current state of the art models of the effect of erosion and roughness on airfoil lift and drag, a benchmark has been undertaken as part of the work package 3 activities that is summarized in a separate report (Campobasso, et al., 2025).

4.1 AEP Erosion Loss Model Components

Modeling AEP loss due to erosion requires capturing the material damage along the blade span, the aerodynamic impact of such distributed and varying damage, the performance impact of the aerodynamic changes on the turbine power curve, and the site wind conditions that drive AEP production. Site conditions also impact hydrometeor damage and the rate of damage are dependent on the combination of turbine operation, wind speed, and hydrometeor characteristics.

The steps in modeling AEP loss can be simplified as:

1.) Spanwise damage model

2.) Aerodynamic Impact of Erosion

3.) Turbine Power Model

4.) AEP Loss

The AEP loss model will be demonstrated on a modern offshore reference turbine: the IEA 22 MW wind turbine reference model (Zahle, et al., 2024). Two examples of modeling AEP loss on this turbine are presented. In both methods, a combination of physical measurements of blade damage from the field, wind tunnel aerodynamic experimental data, and modeling of rotor performance is used to model the power and AEP loss due to erosion. These example modeling methods represent the current state of the art on modeling AEP loss and highlighting where continued work is needed toward a standardized modeling method.

4.2 Sandia Model Description and Results

The first example model of erosion AEP loss for the IEA 22 MW turbine is based on a similar method used on a smaller rotor model by Sandia National Laboratories (Maniaci, et al., 2020).

The Sandia erosion aerodynamic model was used with OpenFAST to simulate turbine performance. Results in previous studies of older, onshore turbine models indicated the wind turbine controller did not change in response to eroded airfoil polars (Maniaci, et al., 2016; Maniaci, et al., 2020), this observation was tested with the IEA 22MW wind turbine OpenFAST model. In addition, this model was used to explore the difference in using a simple constant value of blade damage on the outer part of the blade versus using a more physical spanwise damage model. Additionally, the effect of different spanwise damage model exponents was explored.

4.2.1. Spanwise Damage Model

A definition of the blade erosion category is needed to map to the local distribution of erosion damage across the blade to assess the rotor AEP loss, requiring the blade damage defined at one location on the blade along with the relative distribution of damage along the remaining blade span. The distribution of blade erosion along the blade span was simulated using the local blade velocity to the 6.7 exponent for erosion, which is slightly higher to the value found in Section 3; however, the exponent can range widely in testing observation (5-10). Erosion damage models have a wide range of complexity, the simple exponential model is meant to capture the rate of damage change along the blade span without the complexity of physics based material damage models (Prieto & Karlsson, 2021).The resulting spanwise damage distributions with the blade category defined at the 98% location are shown in Figure 7.

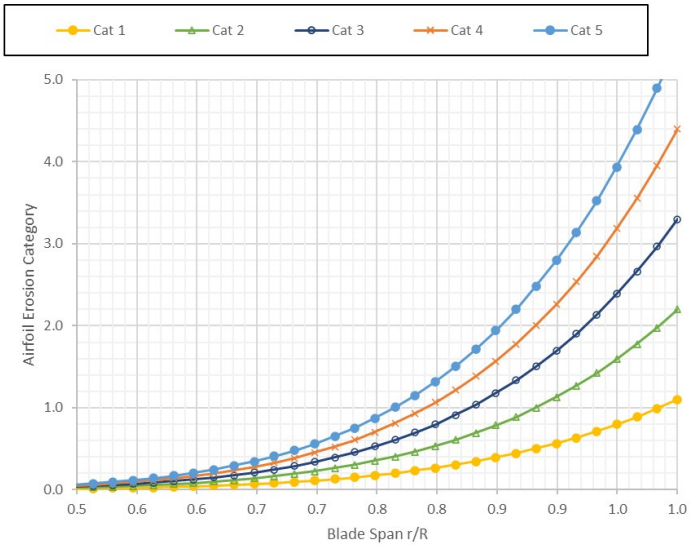

Figure 7. Spanwise damage model for the erosion category proportional to the incoming velocity at each blade section to an exponent of 6.7 ($V_s^{6.7}$).

A simplified spanwise damage model was created to limit the number of airfoil polars with blade damage to five integer values, following assumptions used in past work (Maniaci, et al., 2020). This simplification was accomplished by defining the blade erosion category by the value at 98% of the blade span and then rounding the spanwise damage model results to the nearest integer value, as shown in Figure 8.

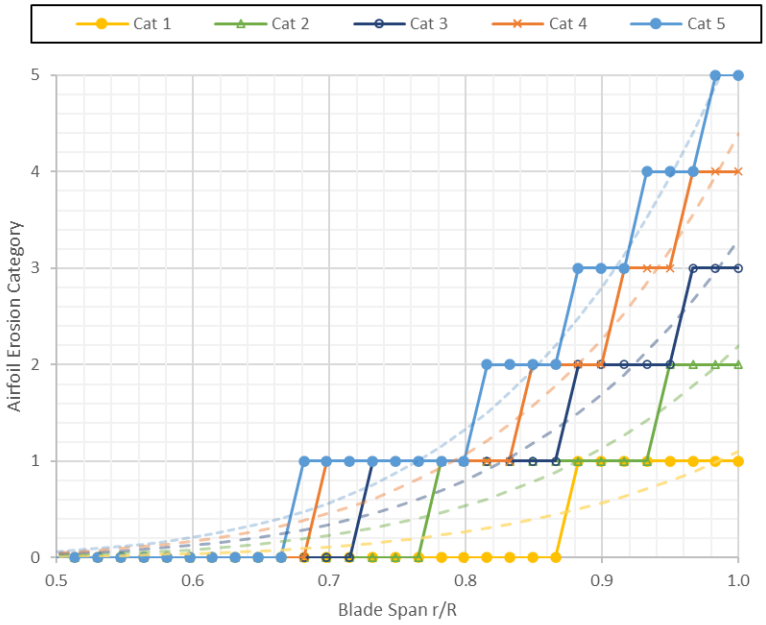

Figure 8. Stair-step simplified spanwise damage model.

The selection of the spanwise damage exponent has a non-negligible influence on the inboard extent of damage. Reducing the exponent to 5.4 ($V_s^{5.4}$) from the 6.7 value used in the other cases while maintaining the blade category definition of category 4 blade erosion at the 98% span location results in damage progressing inboard by an additional 10% over the other cases, as shown in Figure 9. This case is termed 'Cat 4 exp 5.4' in the power results.

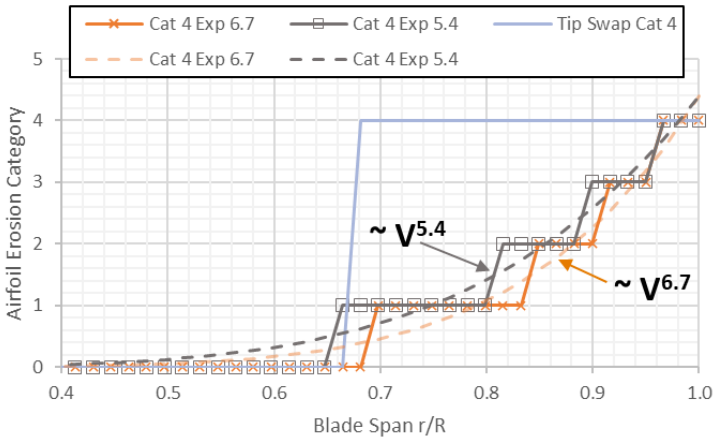

Figure 9. Impact of exponent in erosion damage model.

The present work defines blade category as when the outer 2% of a blade is at or above the blade erosion category (Maniaci, et al., 2025), previous work defined it as

the outer 5% (Maniaci, et al., 2020). This difference of defining the blade erosion category by the 98% blade spanwise location versus the 95% location changes the AEP loss mapping by an entire blade category: Category 5 blade loss in the new system is like Category 4 blade loss in the old system. This work highlights the need for a common blade erosion category system, which is planned for future work in collaboration between the task work packages.

4.2.2. Aerodynamic Impact of Erosion

Leading edge erosion reduces the lift production of a wind turbine airfoil for a given angle of attack and increases the drag, together reducing the lift to drag ratio. The most accurate way to estimate the lift and drag production of a wind turbine airfoil is in a wind tunnel test, where the turbulence in the natural wind can be limited to increase measurement accuracy. In order to measure the effect of actual leading edge erosion damage on aerodynamic forces, past work relied on taking impressions of blade damage from a section of a blade identified as category 4 erosion on a 1.5 MW class wind turbine, as shown in Figure 10 (Ehrmann & White, 2015) (Maniaci, et al., 2016). These impressions were then scaled and reproduced through three-dimensional printing to create a modified airfoil model that could be tested in a wind tunnel (Ehrmann & White, 2015). Wind tunnel tests of the replicated erosion on the NACA 63_3-418 airfoil were performed at the Texas A&M Oran W. Nicks wind tunnel (Ehrmann, et al., 2013) (Ehrmann & White, 2014).

Figure 10. Field measurements and wind tunnel test of Cat 4 erosion (Ehrmann & White, 2015) (Maniaci, et al., 2016)

The results of the wind tunnel tests from Texas A&M (TAM) are shown in Figure 11, with the eroded leading edge case (ELE) representing the category 4 erosion reproduction. The ELE case shows both a larger increase in drag and decrease in lift than the case where the flow was tripped, both at and above the design lift coefficient.

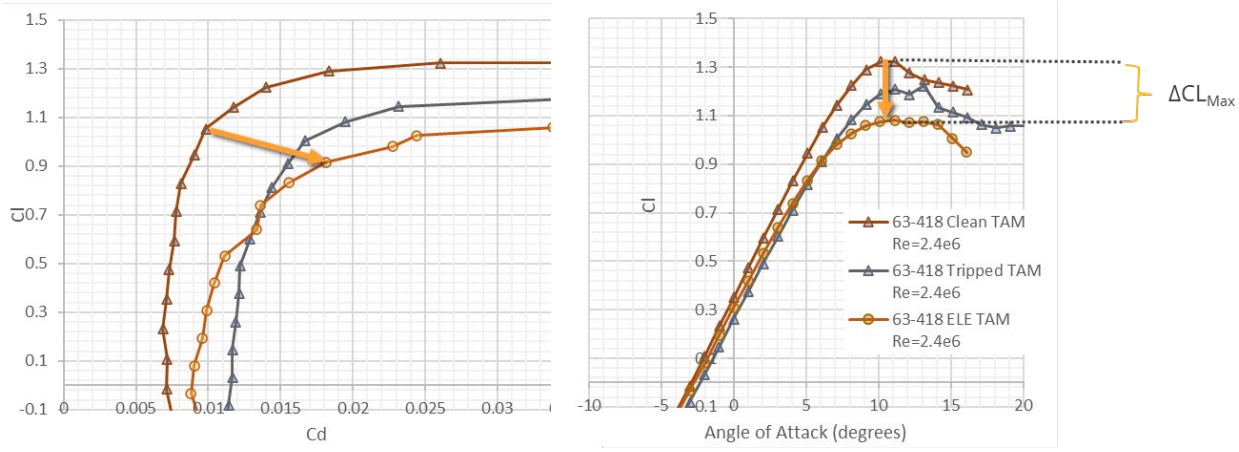

Figure 11. Lift and drag change with erosion on the NACA 63_3-418 airfoil based on wind tunnel tests of 3D printed category 4 erosion reproduction.

In previous work, it was desired to simulate the effect of erosion on power production for a rotor that uses a different airfoil than the wind tunnel test, the National Rotor Testbed (NRT) rotor, which uses the S825 airfoil at the blade tip (Kelley, 2015). A method was developed to take the change due to erosion on the aerodynamic characteristics of the wind tunnel measured NACA 63_3-418 airfoil and apply them to the desired S825 airfoil (Maniaci, et al., 2020). This method has been further developed to normalize the effect of erosion and apply the normalized corrections to the FFA airfoils used outboard in the IEA 22 MW wind turbine model. The change in lift and drag due to category 4 erosion from the wind tunnel tests of the NACA 63_3-418 were normalized by the stall angle-of-attack and applied to the FFA airfoils . This polar modification method for category 4 erosion resulted in a 12% loss in lift at the design CL (max L/D clean), 19% loss in lift at CL_{Max}, 77% increase in drag at design CL, and 141% increase in drag at CL_{Max}, with an overall ~50% reduction in maximum lift to drag ratio. The additional categories of erosion (1-3) were defined through linear interpolation of the lift and drag polar data, with the resulting modified polars shown in Figure 12 and Figure 13.

The impact of erosion on stall margin (difference between angle of attack for maximum lift and for the design lift) was not included in this model based on the wind tunnel results from the NACA airfoil; however, more recent wind tunnel tests from the DTU LERCat project indicate that stall margin should be added as a parameter in the future.

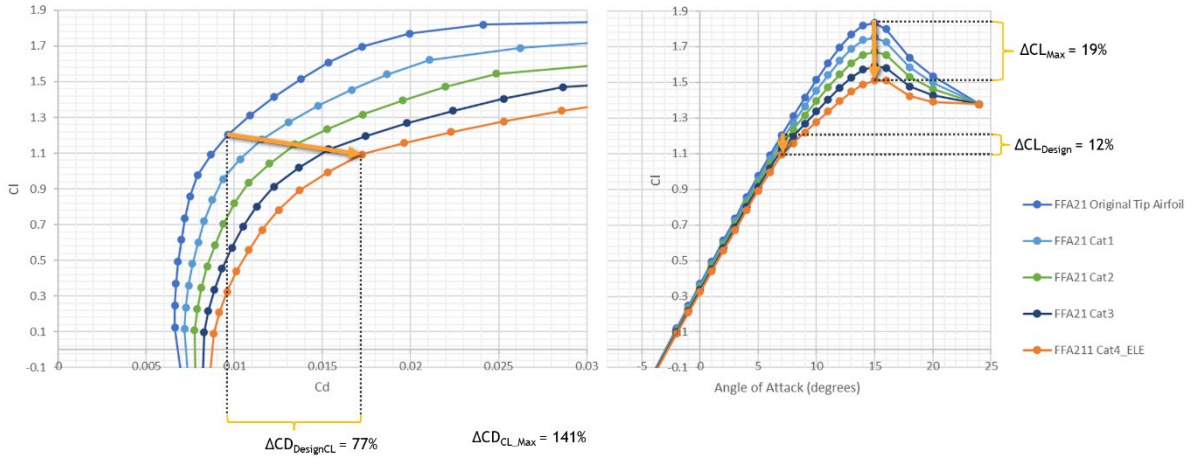

Figure 12. Airfoil polar with erosion correction: FFA-W3-211.

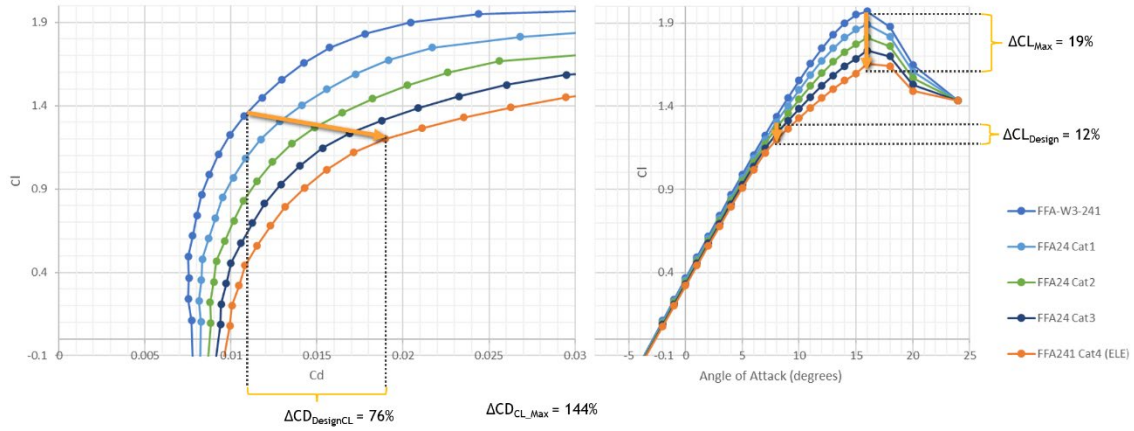

Figure 13. Airfoil polar with erosion correction: FFA-W3-241.

4.2.3. Turbine Power Model

The spanwise damage model is used to distribute the eroded airfoil polars according to the damage class to create an aerodynamic model of an eroded blade. To simulate the power loss due to erosion, the eroded blade model is then simulated with blade element momentum theory in an aeroelastic rotor modeling code, OpenFAST. These simulations were performed with steady wind (Windtype = 1) with a 0.12 shear power law exponent. A simpler model of the effect of erosion on blade aerodynamic performance was also created where the detailed damage across the blade span was ignored and the outer two airfoils were swapped for the category 4 erosion polars. The resulting modeled power curves from the range of simulated cases is shown in Figure 14. The Baseline case is the rotor with the clean airfoil polar data, representing an idyllic state of the turbine with ideal blades that are perfectly clean, this case is used as the reference case with the relative power loss in Figure 15.

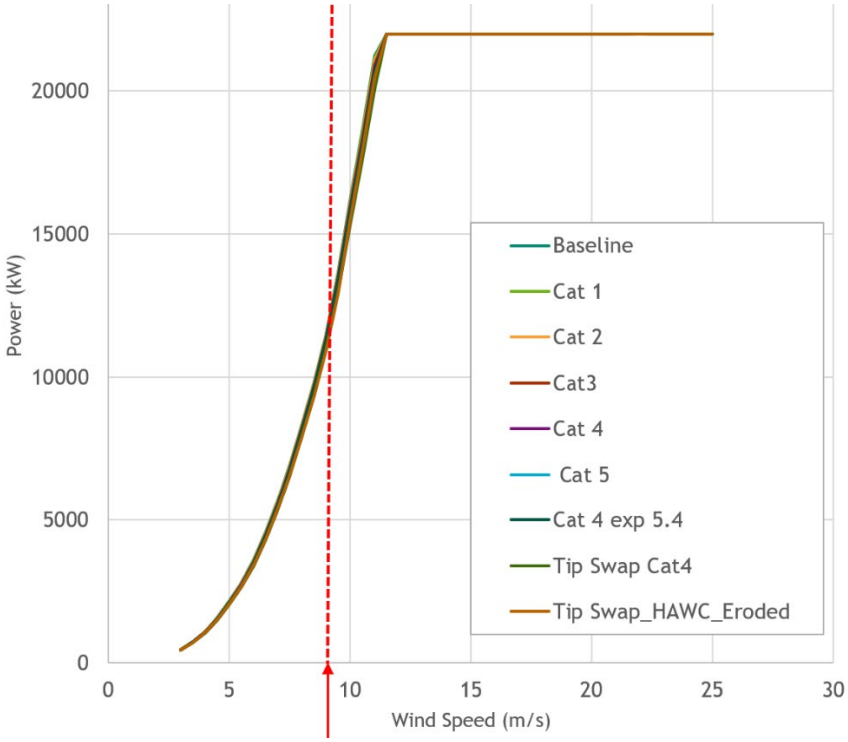

Figure 14. Power curve with erosion of IEA 22 MW wind turbine.

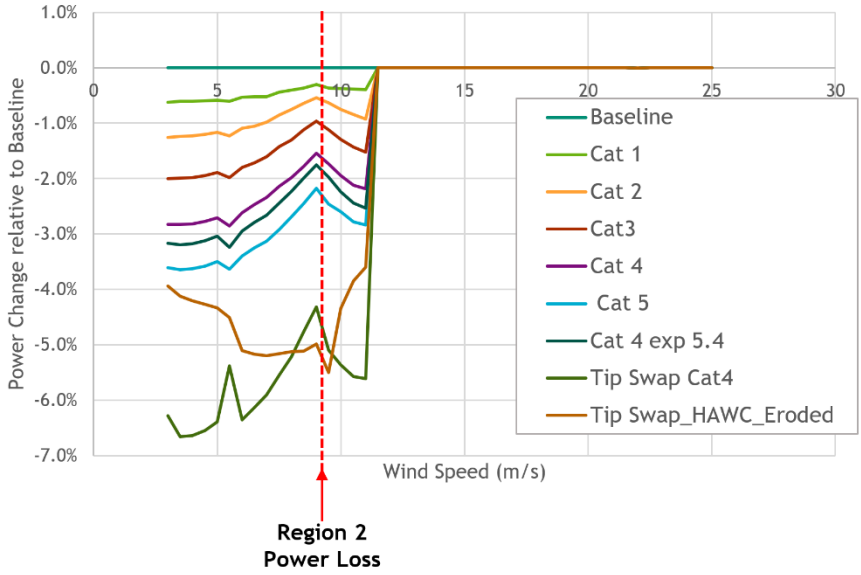

Figure 15. Power loss versus wind speed for range of erosion cases.

The blade erosion damage distribution defined in Figure 8 define the Cat 1 through Cat 5 cases in Figure 14. Decreasing the spanwise damage exponent to 5.4 ($V_s^{5.4}$) in the 'Cat 4 exp 5.4' case decreased power production an additional 14% over the 'Cat 4' case with a 6.7 exponent. The highest reduction in power production is observed with the case where the outer two airfoil polars were swapped with the category 4 polars ('Tip Swap Cat4' defined in Figure 9). The simple airfoil polar swap method was also applied with the simulated eroded polars used in the DTU studies of the IEA 22 MW, described later in this report, for comparison to the OpenFAST results.

The power loss at the top of region 2, where the turbine is still at its optimum tip-speed ratio, can be a useful reference point and is shown in Figure 16. In the past study of the effect of erosion on power and AEP of the NRT rotor (Maniaci, et al., 2020), the power loss fairly constant near the top of region 2 operation, and so this was seen as a potential point to compare the effect of erosion between turbines. However, the power loss results for the IEA 22 MW turbine are not as consistent across region 2 operation in the OpenFAST simulation results, for both the polar modification method presented in this section as well as for the DTU polars used in the HAWC simulations. The reduction in power loss near the higher end of region 2 in the OpenFAST simulations is likely due to the pitch controller being active in region 2 in the IEA 22 MW turbine model, whereas in the NRT modeled used in previous work the pitch is constant in Region 2 operation. Future work will include investigating the impact of pitch control with the eroded airfoil polars along with including the impact of adding a model for the reduction on stall margin to the polar modification method.

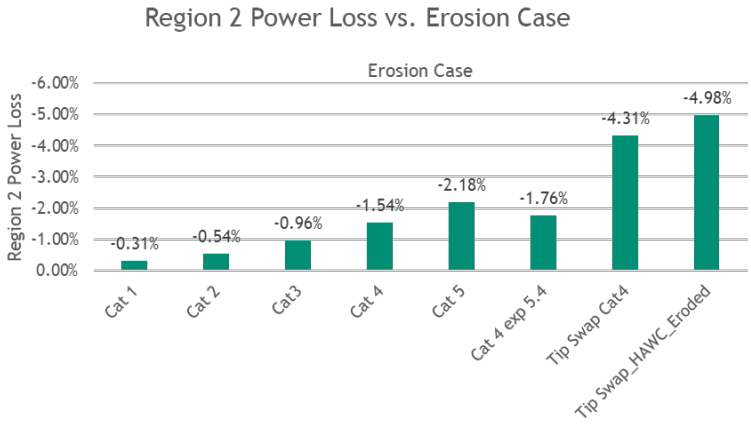

Figure 16. Region 2 power loss for range of erosion cases.

4.2.4. AEP Loss

The power loss predictions for the IEA 22 MW turbine were used with a Rayleigh wind distribution with 8.5 m/s mean wind speed to estimate AEP loss, as shown in Figure 17. The cases where the outer two airfoils were swapped for category 4 erosion polars showed the highest predicted AEP loss of about 2%, while the case with category 5 erosion at the blade tip with the modeled damage distribution resulted in about 1.2% AEP loss.

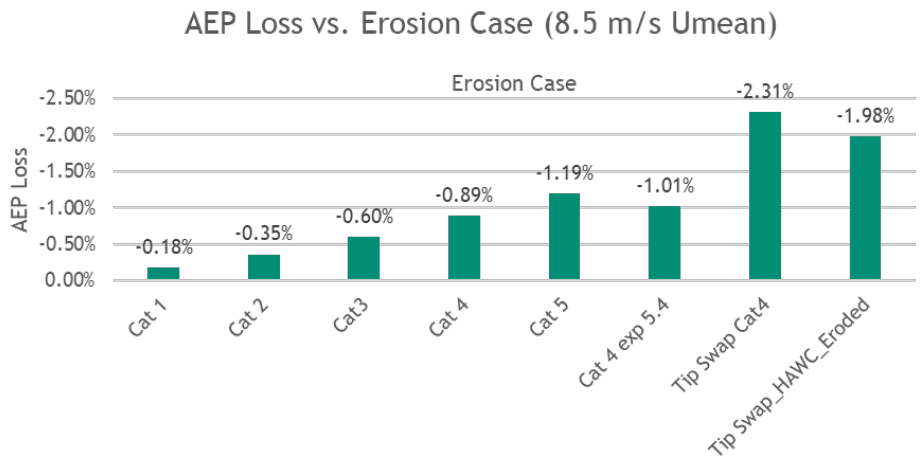

Figure 17. AEP loss for range of erosion cases, 8.5 m/s mean wind speed.

These AEP loss predictions for the IEA 22 MW wind turbine are on the low side of expected values and are lower than previous studies, likely due to the decreased loss near the top of region 2 operation. Since full-scale validation of these results is not possible, sensitivity studies and code-code comparisons are planned, along with assessing what the requirements would be for a validation experiment.

4.3 DTU Erosion Loss Modeling of the IEA 15 and 22 MW

At DTU the open-source Simplified Aerodynamic Loss Tool (SALT) has been developed (Bak & Meyer Forsting, 2023) to provide fast estimates of AEP loss due to changes in the sectional aerodynamic performance of blades. The model is based on BEM and only requires a very limited set of turbine specific inputs, namely the specific power, rated wind speed and tip speed ratio: sectional aerodynamic losses can be specified over any section of the blade span. An essential assumption of SALT is that the turbine operates at the optimal tip speed ratio below rated wind speed, thereby maintaining constant design lift and drag coefficients throughout, and is aerodynamic loss agnostic, i.e. the operation of the turbine remains unchanged despite changes in lift and drag along the blade span. In the original publication of SALT (Bak, 2022), power loss predictions seemed in-line with those by steady-state BEM for the Vestas V52 turbine (R=26m, 850kW). Whether this also holds for larger turbines and in more realistic inflow with shear and turbulence, will be explored in this section. For this purpose the IEA 15 MW (Gaertner, et al., 2020) and IEA 22 MW (Zahle, et al., 2024) offshore reference turbines are simulated with erosion losses in HAWC2, a high-fidelity aeroelastic solver, in uniform and turbulent, sheared inflow and compared to SALT predictions. A focus lies in identifying how turbulence and the turbine controller settings affect erosion losses.

4.3.1 Turbine Definitions

The IEA 15 MW and IEA 22 MW reference turbines (see Figure 18), are modern offshore wind turbine designs for which full aero-hydro-servo-elastic models are openly available. This includes controllers and airfoil data, which allows exploring the effects on AEP and rotor operation, due to changes in the sectional aerodynamic

performance from LE roughness and erosion. Below rated wind speed, where the adverse effects from LE damage are expected to be largest, the turbines operate quite differently, with IEA 15 MW blade operating at lower angles-of-attack, which is expected to lead to lower power losses, and thus an interesting contrast to the more conventionally operating IEA 22 MW.

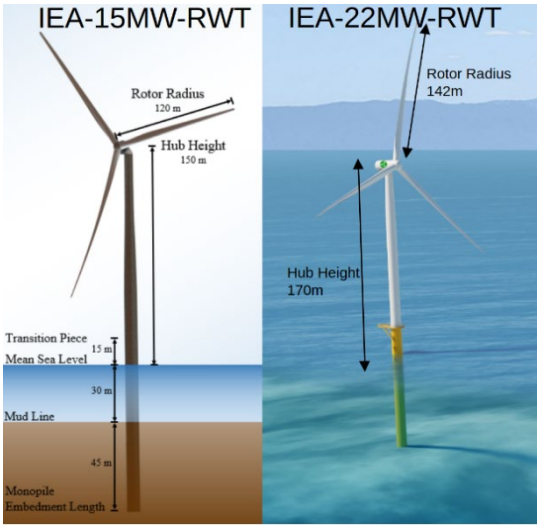

Figure 18: Dimensions of the IEA 15 MW and 22 MW offshore turbines.

4.3.2 Aerodynamic Modelling of Erosion

The aerodynamic definition of the rotor blades is provided through the airfoil family employed and the radial relative thickness distributions. Both turbines use the FFA-W3 airfoil family; however, their thickness distributions differ as shown Figure 19, with the IEA 22 MW only employing the 21.1% thick airfoil at the very tip. As shown by the analysis of spanwise damages observed in the field (see Section 3), mostly the outer 40% of a rotor suffers from extensive LE damage. In this region both turbines use the 21.1% and 24.1% airfoils, their spanwise positions are indicated in Figure 19. Hence, to study the effect of aerodynamic performance changes over this region of the blade on power production and turbine operation, the original 2D polar data of these two airfoils is modified.

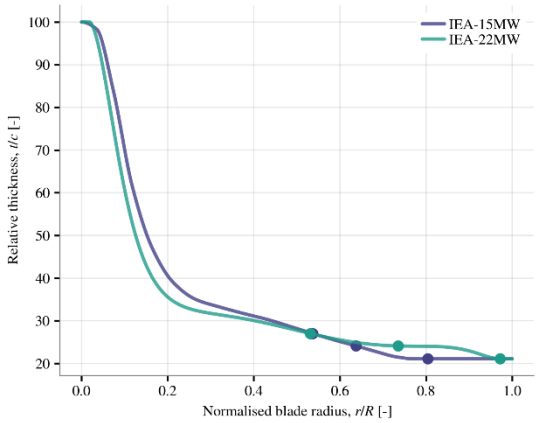

Figure 19: Relative thickness distributions of the IEA 15 and 22 MW offshore turbines, with dots indicating the positions of the 21.1%, 24.1% and 27.0% airfoils from the FFA-W3 airfoil family.

As the thickness distribution is used to interpolate in-between the provided airfoil data, both turbines' aerodynamic coefficients differ from the original for the outer half of the blade, i.e. r/R > 0.53, the position of the 27.0% thick airfoil. Yet as the two turbines employ different shares of the two airfoils in the outer blade region, they will be affected differently by updates to the airfoil data.

The original airfoil polars were generated by 2D CFD simulations using DTU Wind's in-house setup relying on the EllipSys2D solver and tools. The same setup is used here, with polars generated at Reynolds numbers of 10 and 16 million for the 21.1% and 24.1% airfoils, respectively, following the definition of the IEA 22 MW. This is a slight change with respect to the original definition of the IEA 15 MW that employs polar data at 10 million everywhere, however this has negligible impact on rotor performance. The original airfoil data of the aeroelastic models is a 70/30 mix of transitional and fully turbulent polars, where the former captures free transition from laminar to turbulent boundary flow by coupling the e^N transition model to the turbulence closure in the CFD model. Fully turbulent CFD simulations correspond to tripping the boundary layer right at the LE, as caused by surface roughness and damage. Mixing those polars ensures that some of the adverse roughness effects are included in the blade design. Previous studies (Ehrmann & White, 2015; Sareen, et al., 2014) showed that LEE forms aerodynamically critical steps close to the LE that degrade airfoil performance far beyond that from tripping the boundary layer alone. Following these investigations erosion like surface damages (Meyer Forsting, et al., 2022) were applied together with a forward-facing step on the suction side at x/c=0.024 of height h/c=0.0015 (c: airfoil chord length) where the damage definitions follow field observations (Ehrmann & White, 2015). The eroded LE is shown in Figure 20 for the 24.1% airfoil. As 2-dimensional damages lead to greater aerodynamic performance degradation than the more realistic 3-dimensional ones seen on blades, these simulations give an upper estimate of the losses expected from severe erosion.

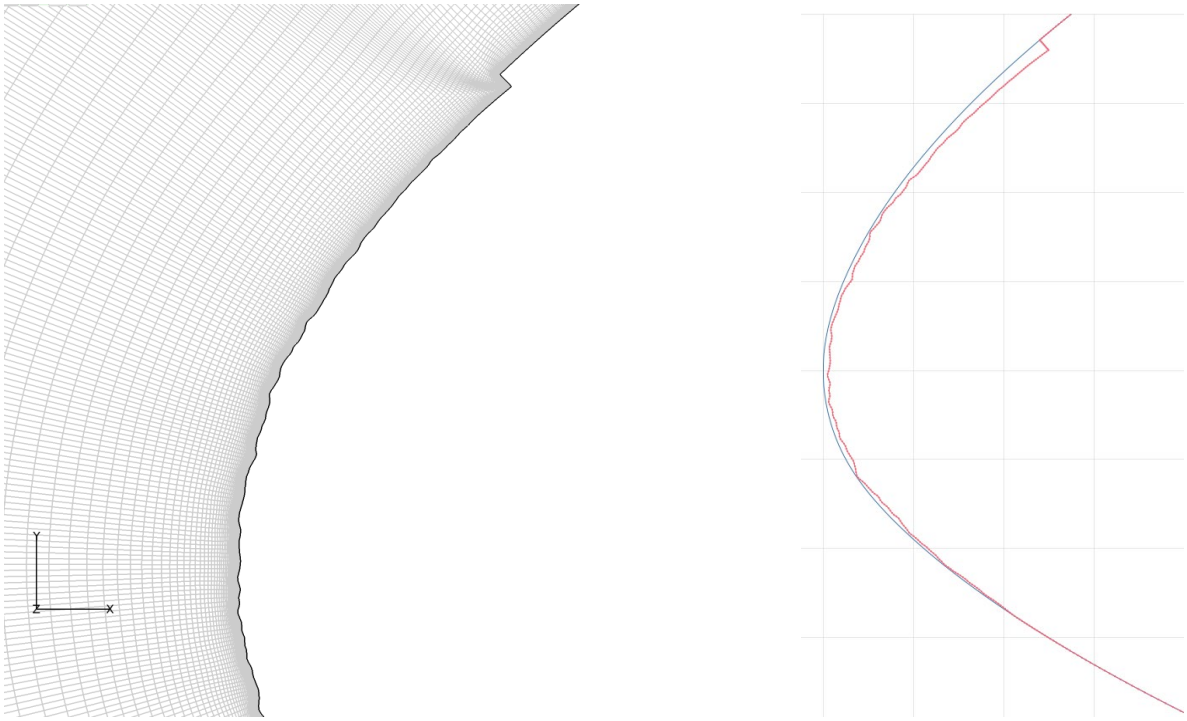

Figure 20: CFD resolved erosion type LE damage on the FFA-W3-241 with a forward-facing step on the suction side at x/c=0.024 of height h/c=0.0015.

The computed performance curves of the airfoils are shown in Figure 21 with the naming definition:

- free transition: Clean airfoil with natural transition
- mixed: 70/30 mix of free transition and tripped
- tripped: Clean airfoil tripped at LE (fully turbulent)
- eroded: Resolved eroded LE (fully turbulent)

Additionally, the change in performance relative to the original polars (mixed) is shown in Figure 22. Whilst the maximum glide ratio for the 21.1% airfoil with free transition is about 10 points higher than for the 24.1% airfoil, it does not differ for the other cases; the maximum just occurs at slightly larger angles-of-attack for the 24.1%. However, the maximum lift coefficient is consistently larger. The stall angle drops by about 4 degrees from free transition to eroded. Whilst the largest marginal drop in glide ratio follows from tripping the boundary layer, this is not the case for the maximum lift coefficient, here it is erosion and not tripping that causes the greatest drop. It is important to note, though, that blades are usually designed and operated such that airfoils operate around the angle-of-attack of maximum glide ratio (here ≤ 9 deg), which should limit losses in lift.

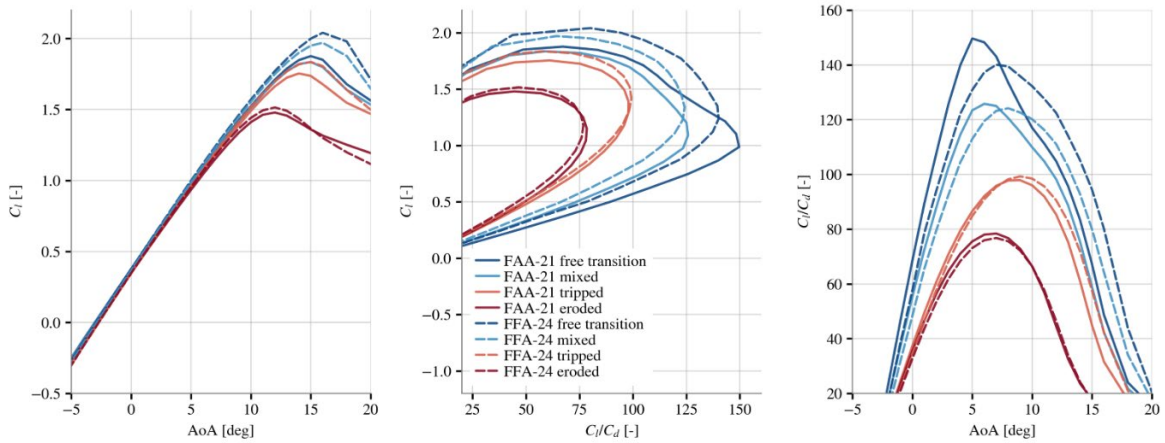

Figure 21: Performance of the FFA-W3-211 (Re=10e6) and FFA-W3-241 (Re=16e6).

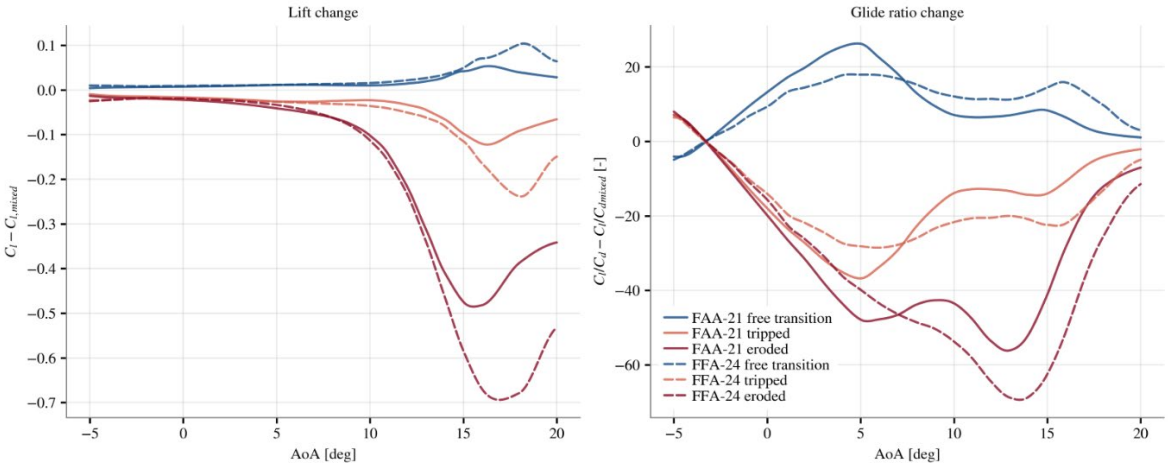

Figure 22: Change in aerodynamic performance with respect to the 70/30 mixed polars.

4.3.3 HAWC2 Simulations

Setup

The aero-hydro-servo-elastic solver HAWC2 is used to simulate the IEA 15 MW and IEA 22MW in normal power production at IEC class IB (V_{av} = 10 m/s, TI_{ref} = 0.14). The converged steady-state response is extracted from time domain simulations without wind shear, turbulence or yaw misalignment (referred to as DLC1.0) and normal power production statistics and fatigue are extracted from DLC1.2 with –8/0/8 degrees yaw misalignment, six turbulence seeds per wind speed and yaw bins, and shear exponent of 0.14 (in total 437 load cases).

Power Curves

The mean power curves from the simulations are shown in Figure 23 for the two turbines, with the naming corresponding to the DLC and airfoil data used. The data is normalized by the nameplate rated power and wind speed values (15MW: 10.59 m/s; 22MW: 11.00 m/s), respectively. Turbulent inflow and shear (DLC1.2) lead to the well documented changes in production also seen here and generally changes in power performance correlate with those in airfoil performance.

To highlight the differences, the change relative to the original rotor using the mixed polars is shown in Figure 24. Changes in power are exacerbated approaching rated wind speed, but quickly disappears once above. Whereas power losses tend to disappear towards cut-in for the 22 MW this is not the case for the 15MW. Whilst the improvement with free transition is limited, the drop due to tripping the boundary layer exceeds 1% and is similar between both turbines. However, once eroded the IEA 22 MW shows greater losses over a wider range of wind speeds.

Turbulence does not fundamentally alter the power loss behavior (compare DLC1.0 to DLC1.2), however it smooths out changes around rated and leads to greater losses for the eroded 22 MW before reaching 0.8 of rated wind speed (coinciding with pitch actuation).

For both turbines the power variability increases significantly above rated when the airfoil performance starts to degrade. The increase is in relative terms higher for the 22 MW turbine, however with respect to rated power they are not dissimilar (not shown).

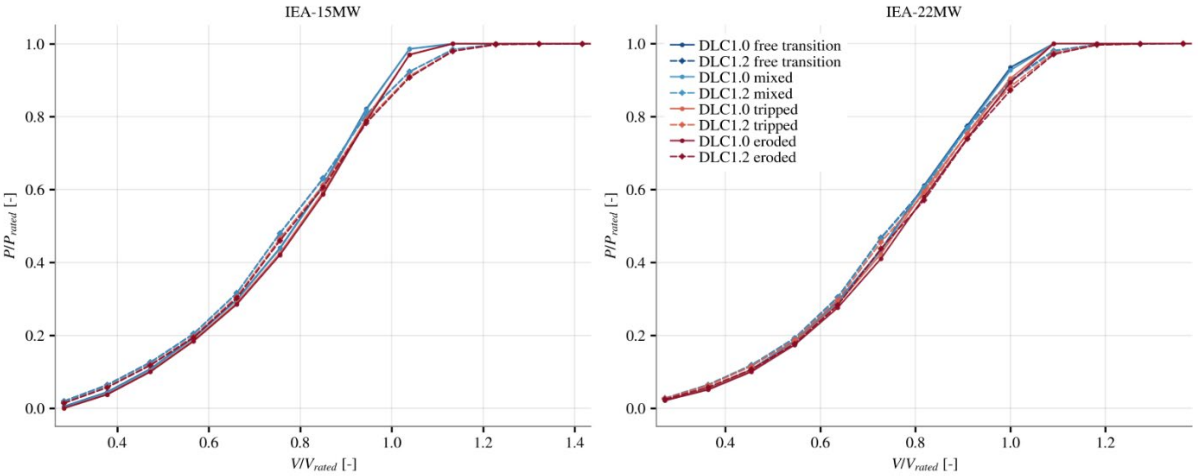

Figure 23: Mean power curves for the IEA 15 MW and IEA 22 MW using different airfoil data for uniform and turbulent inflow.

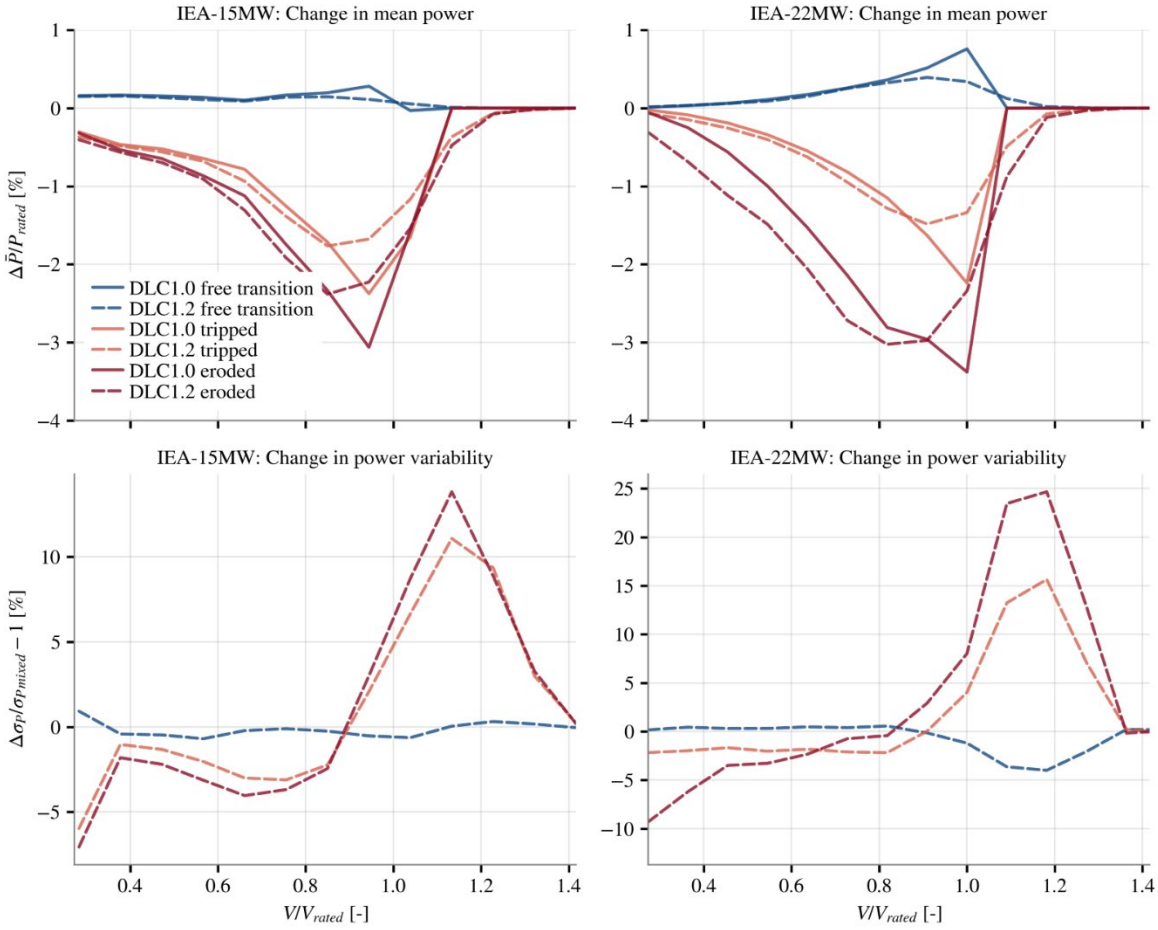

Figure 24: Change in mean power (normalized by rated) and its variability relative to the original power curve using the mixed polars.

Rotor Speed and Pitch

How the turbine controller responds to changes in airfoil performance is explored in Figure 25 by showing the percentage change in rotor speed and absolute pitch angle with respect to the turbine with the original, mixed polars. In terms of rotor speed, little changes are observed for the IEA 15 MW and they occur over a very limited wind speed range (due to an extended constant minimum rotor speed region), whereas the 22 MW responds over the entire below rated region. Changes in airfoil

performance are generally mirrored in the rotor speed (lower driving force -> lower rotor speed). As with power production, turbulence has little influence on rotor speed, except for the eroded 22 MW.
Because pitch actuation is limited for both turbines below 0.8 of rated wind speed (only tracking minimum pitch settings), changes only occur above. Actuation does not vary significantly with turbulence, however with degraded airfoil performance pitch to feather (load shaving) occurs at higher wind speeds compared to the baseline. The difference persists above rated, as the controller tries to maintain rated power.

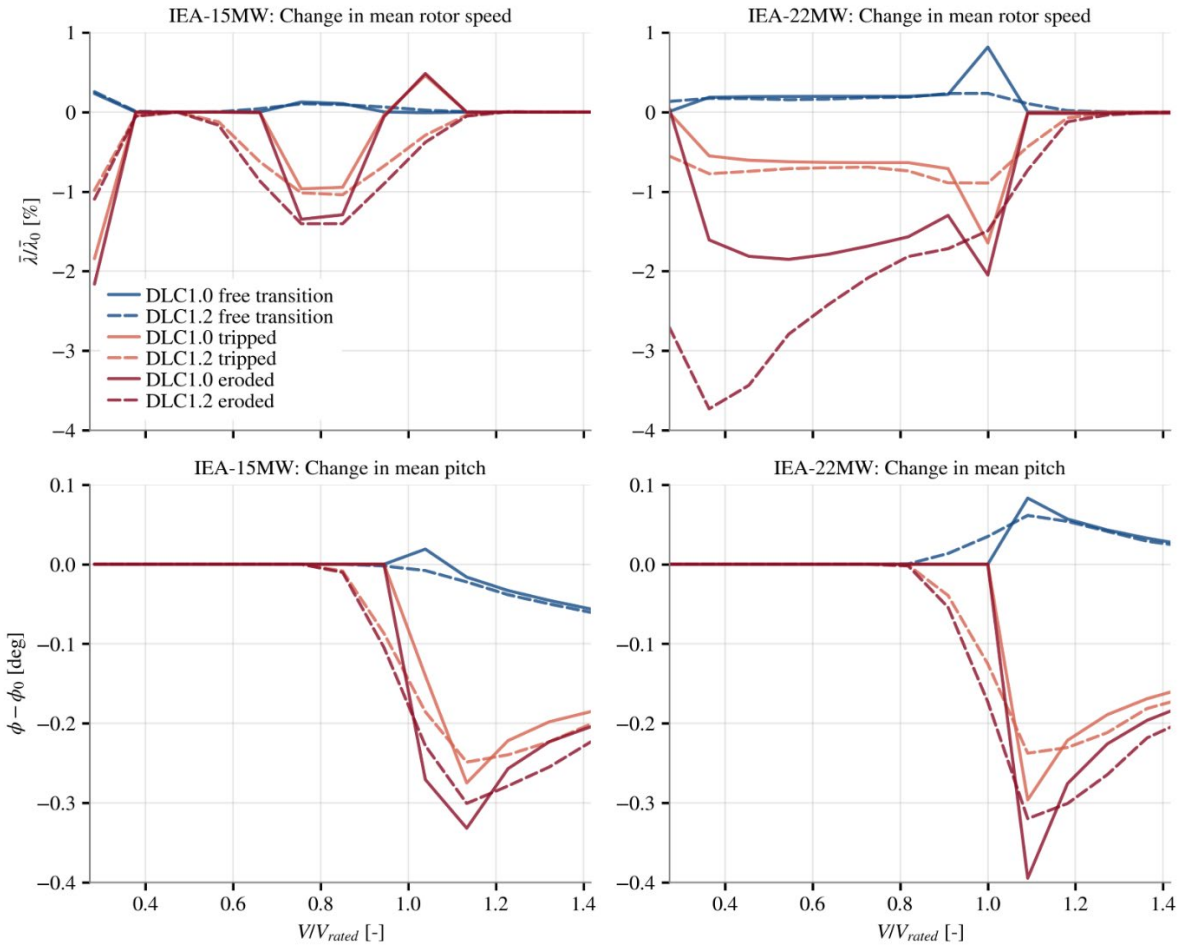

Figure 25: Change in rotor speed and pitch with respect to the original power curve using the mixed polars. Positive pitch to feather.

Angles-of-Attack

The changes in power observed in Figure 24 and differences between the rotors can be related to the changes in the angle-of-attack at which sections along the blade are operating. The variation of angle-of-attack and lift coefficient with wind speed for sections at 90% of radius are shown in Figure 26. In case of the IEA 15 MW this section operates at 0.5º below most of the outer blade region (radially near constant angle-of-attack) when below rated, whereas for the 22 MW it peaks at this position (rises by about 1.5º from r/R=0.6 to its peak at r/R=0.9).
Clearly both rotors operate at very different angles-of-attack below rated with the IEA 22 MW operating more conventionally, keeping the angle-of-attack constant and thereby the airfoils close to maximum glide ratio (max. for mixed 21.1% at 6º; mixed

24.1% at 8º). Generally, the angle-of-attack increases as airfoil performance degrades, as the rotor tries to recover lift. Whereas this is achieved by the IEA 15 MW, the 22 MW cannot achieve the target lift (about Cl=1.5) when eroded, as the airfoil starts to stall (refer to Figure 21); especially an issue at lower wind speeds. Mean values with non-turbulent inflow are generally above those with turbulence, however the changes with respect to the mixed are generally similar. Whether those patterns persist over the entire blade span is investigated in Figure 27. It presents the changes in angle-of-attack and lift along the blade with respect to the original rotor at 0.58 of rated wind speed (around the peak in Figure 26 seen for the IEA 15 MW). The angle-of-attack and lift are clearly altered over the outer region of the blade for which the airfoil polars were modified (r/R>0.53). Here again the eroded 22 MW clearly stands out, with significantly greater increases in angle-of-attack, which are accompanied by large drops in lift towards the tip, as the outer part of the blade starts to stall. It is also worth highlighting that the inner part of the blade, unaffected by airfoil changes, recovers some of the loss in lift.

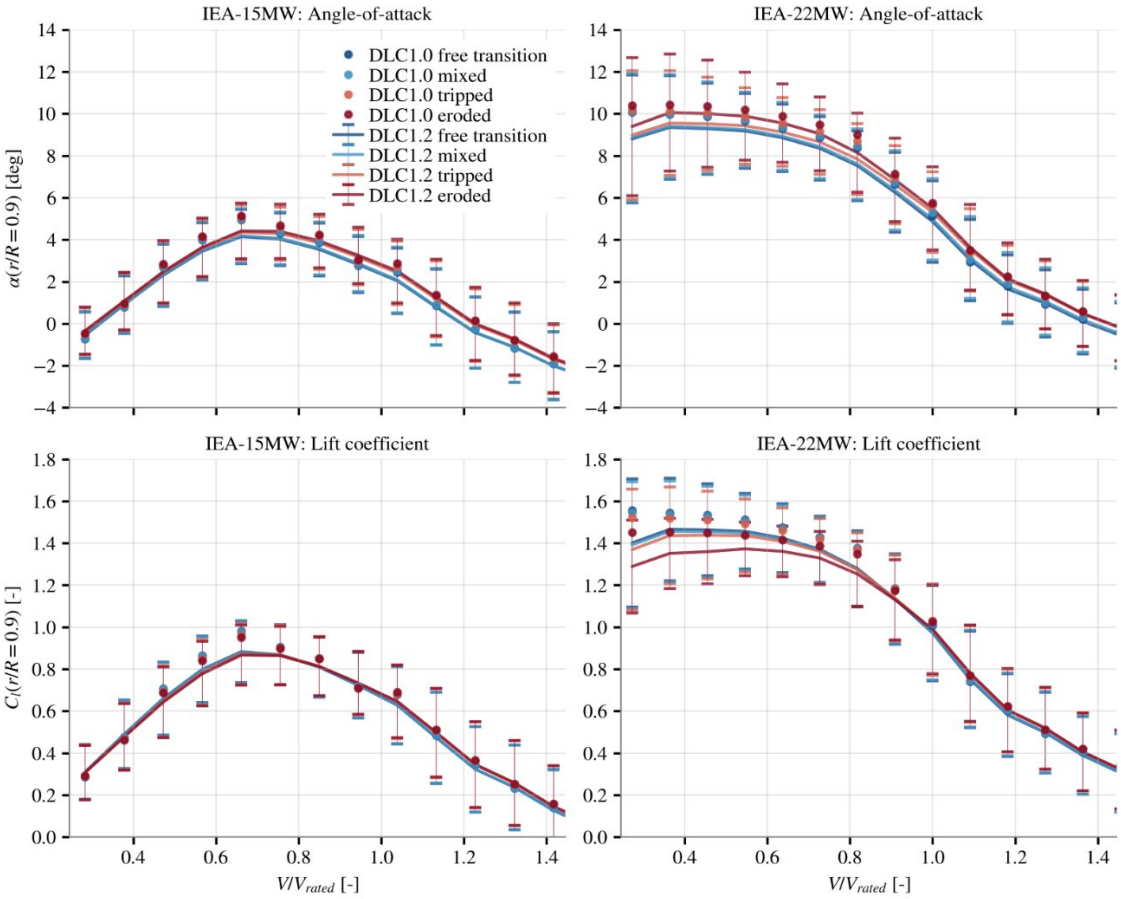

Figure 26: Angle-of-attack and lift coefficient variation with wind speed at sections at 90% of radius.

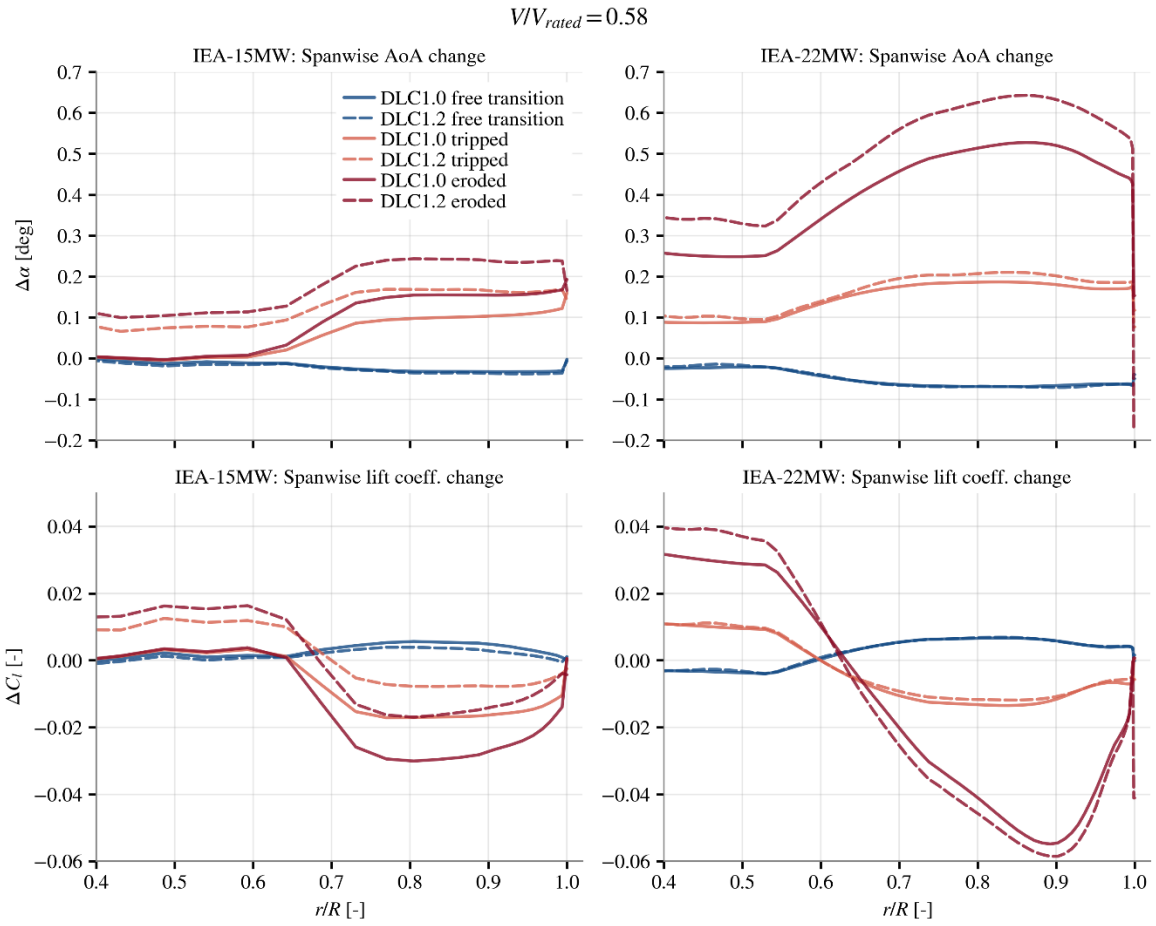

Figure 27: Changes in radial angle-of-attack and lift coefficient distributions at 0.58 of rated wind speed with respect to the original turbines using mixed polars.

4.3.4 SALT vs HAWC2 AEP Loss Predictions

SALT Setup

The simple model only requires a very limited number of inputs, most of which can be directly taken from the definitions of the reference turbines. The aggregated inputs are listed in Table 3, where the design lift was estimated from the HAWC2 results for the outer half of the blade.

Table 3: SALT turbine inputs

	IEA 15 MW	IEA 22 MW
Rated elec. power [W]	15e6	22e6
Rotor radius [m]	120	142
Cut-in wind speeds [m/s]	3	3
Cut-out wind speeds [m/s]	25	25
Max. tip speed [m/s]	95	105
Opt. tip speed ratio [-]	9	9.153
Drivetrain efficiency [-]	0.965	0.954
Design lift coefficient [-]	0.8	1.5

Furthermore, it requires the radial distribution of lift-to-drag from the clean blade, and radial loss factors (fraction of clean). Here the ‘clean’ distribution is found by finding the maximum lift-to-drag ratio at each radial station of the original rotor (mixed

polars) and evaluating the other blades at the angle-of-attack for which the maximum was found. This is meant to mimic aerodynamically optimal rotor control, which tracks the maximum lift-to-drag ratio (constant sectional angle-of-attack) below rated wind speed but does not adapt to changes in sectional aerodynamic performance. The resulting radial distributions for the different rotors are given in Figure 28. As the IEA 15 MW controller does not track maximum glide ratio below rated, distributions were also created by extracting lift-to-drag ratios 2º below the one giving the maximum (dash-dotted lines). The fractions of lift-to-drag ratio can readily be computed from those distributions and fed into SALT to compute power losses.

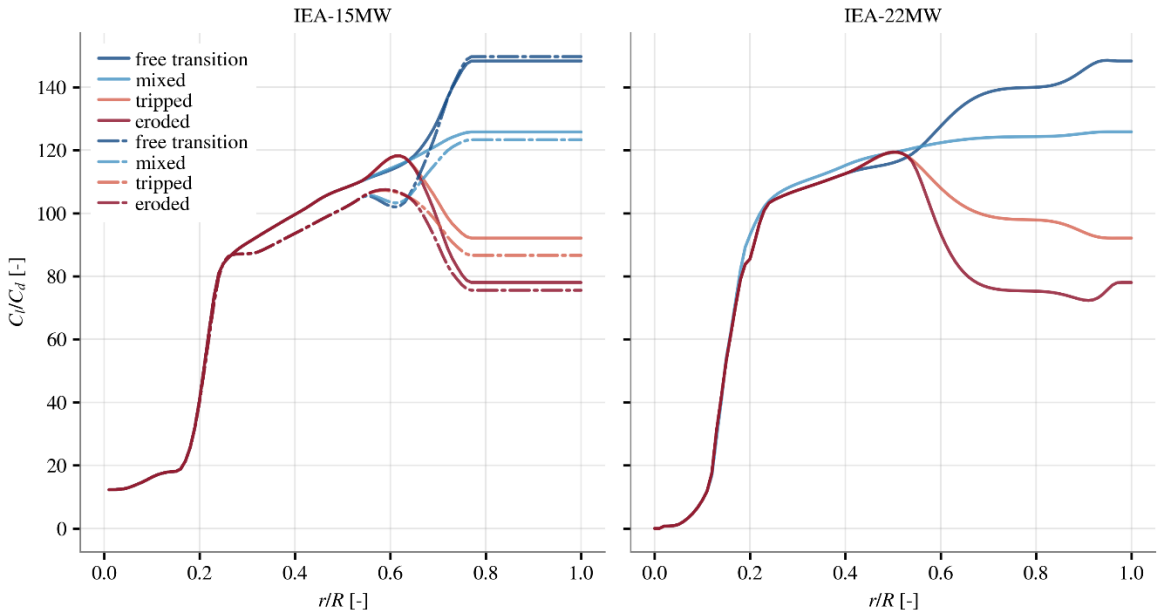

Figure 28: Radial lift-to-drag ratio distributions. Dash-dotted lines indicate glide ratios extracted at angles 2º below maximum.

Power Loss and AEP Predictions

The predictions by SALT are compared in Figure 29 to those by HAWC2 with uniform inflow (DLC1.0), as those align with the steady-state assumptions of SALT. Dash-dotted lines for the IEA 15 MW correspond to glide ratios extracted at lower angles-of-attack. As SALT is only meant to capture losses, it is not surprising that it does not predict gains. The agreement below 0.8 of rated wind speed is rather good for the IEA 22 MW, whilst around rated, where the turbine starts to pitch and de-load, they diverge. Generally, HAWC2 predicts losses beyond rated wind speed, which is not the case for SALT. Whilst computing the lift-to-drag ratio at lower angles-of-attack, brings the predictions more in-line, there remain large differences at lower wind speeds.

The reason for those differences can at least in part be attributed to differences in the tip speed ratios shown in Figure 30. SALT only takes the optimal tip speed ratio as input and assumes that it is maintained below rated, however both turbines diverge from this assumption towards cut-in and rated wind speeds. The 15 MW especially deviates from this assumption at lower wind speeds, as it enforces a relatively high minimum rotor speed. Whenever the rotors do operate at or close to optimum tip speed, the agreement with SALT improves.

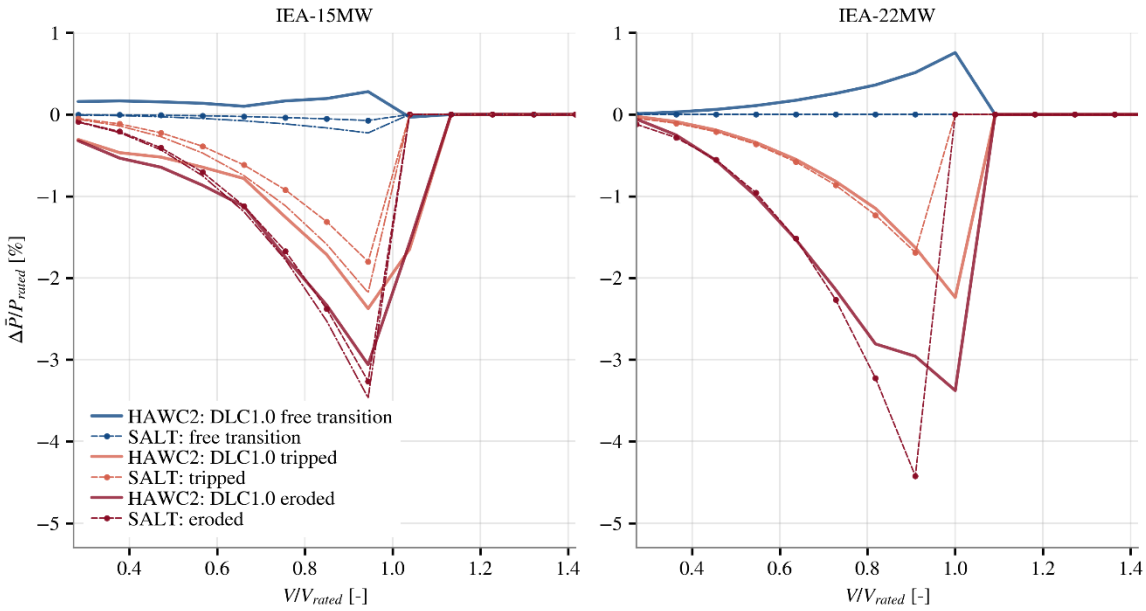

Figure 29: Comparison of power loss predictions by HAWC2 with uniform inflow and SALT

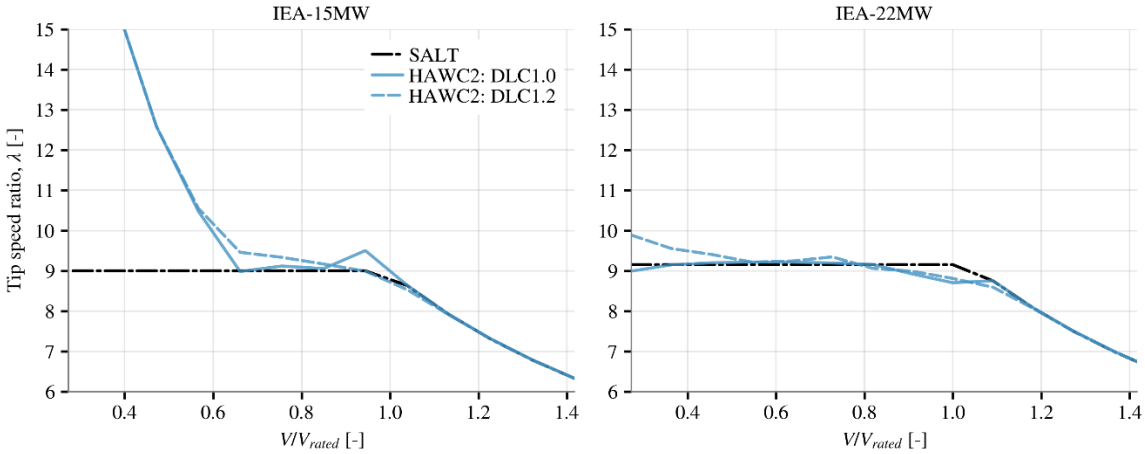

Figure 30: Tip speed ratio curves from different models.

Table 4 shows the changes in AEP predicted with respect to the mixed baseline using a Weibull wind speed distribution with parameters corresponding to the turbine class. Whilst differences have been observed between idealized (DLC1.0) and operational (DLC1.2) HAWC2 results, the differences in terms of AEP change are negligible, as differences cancel out. However, the two turbines differ significantly in their response. The losses from tripping the boundary layer are lower on the 22 MW than on the 15 MW, but suffers significantly more from erosion. The reason for this behavior can be directly linked to changes in sectional aerodynamic performance (refer to Figure 22). Tripping has a larger influence on the 15 MW as it is operating at lower angles-of-attack, 5º versus 8º on the 22 MW, where the loss in glide ratio is much larger. The loss in lift coefficient is about the same, though. Yet, when the airfoil is eroded, the drop in glide ratio is similar, but the loss in lift quickly increases with angle-of-attack. SALT generally underestimates AEP losses, as it does not capture the power losses around rated wind speed correctly. Here the aerodynamically sub-optimal operation of the turbines plays a role. Whether changing the tip speed curve within SALT would remedy the underprediction should be tested.

Table 4: Predictions of AEP changes in %. Parentheses indicate IEA 15 MW simulations with L/D distributions below optimal. (Weibull parameters: k=2, A=11.3 m/s).

IEA 15 MW	HAWC2 ideal	HAWC2 operational	SALT
mixed	-	-	-
free transition	+0.14	+0.11	-
tripped	-1.13	-1.09	-0.64 (-0.78)
eroded	-1.43	-1.45	-1.16 (-1.24)

IEA 22 MW	HAWC2 ideal	HAWC2 operational	SALT
mixed	-	-	-
free transition	+0.27	+0.21	-
tripped	-0.84	-0.85	-0.61
eroded	-2.07	-2.10	-1.60

5. Future Work

The work planned in Phase 2 of IEA Wind Task 46 will build off the AEP loss modeling methods presented in this report. Three of the main activities that will continue to advance the modeling of AEP loss are listed here:

1. Updated erosion classification system with report, collaboration across work packages with recent participant results:
    - Based on LERCat and WP4 developments;
    - Look at correlation between field observations of erosion and erosion test stand results;
    - Look at erosion test stand power demand changes as erosion progresses; and
    - Also, look at correlating erosion categorization with inboard progression of damage/incubation.

2. Aerodynamic benchmarking and simulations, and reference models:
    - Aerodynamic benchmark on LERCat data;
    - Relate erosion categories to sandgrain roughness or other roughness parameterization. Application to canonical erosion progression (Springer model) along with actual observations of erosion;
    - Predict how higher Reynolds numbers (2-3 times wind tunnel tests) will impact aerodynamics of roughness and erosion, design experiment to address data gaps; and
    - Modelling and benchmark on aerodynamic effects and loss due to several representative LEP solutions.

3. Annual energy production (AEP) Loss and Reference Erosion Turbines Models:
    - Reference turbine models for a range of modern turbine types for the prediction of annual energy production loss based on blade erosion class or actual observations of erosion;
    - Model uncertainty in AEP loss predictions based on ideal erosion classification and realistic uncertainty in classification;
    - Include a range of roughness, erosion, and LEP in the results; and
    - Development and publication of simple AEP loss models for the reference turbines, applied to a range of wind sites.

6. Conclusions

This report shared methods used to model the annual energy production (AEP) loss due to leading edge erosion. The relationship between blade erosion categories and AEP loss is of practical interest to those relying on the power production of wind turbines and is still a critical source of uncertainty in model predictions. Spanwise damage distribution definition methods are also very important for accurate AEP loss predictions, and future work is needed to have a model that can be easily related to material test data. The current state of the art in predicting AEP loss is to use either calibrated computational models of the effect of erosion on airfoil force data or to use high quality wind tunnel measurements of such effects, both methods are utilized in this report, showing how a combination of wind tunnel and modeling results is effective. The IEA15 MW and IEA 22 MW reference wind turbines were selected as modern erosion reference models and two approaches were presented to simulate the impact of erosion on its power and AEP production. The results showed different trends than past work, in part attributed to the active pitching of the IEA 22 MW turbine controller in region 2 operation. Furthermore, the effect of turbulence and sheared inflow on relative loss in AEP was minimal and the IEA 15 MW and 22 MW show distinctly different responses to erosion, as they are operated differently below rated wind speed. This work will continue in phase 2 of IEA Wind Task 46, targeting standardization of many of the required modeling methods for AEP loss prediction, continued benchmarking of the models, and exploration of the effects on a range of turbine models and site conditions.

References

Bak, C., 2022. A simple model to predict the energy loss due to roughness. *Journal of Physics: Conference Series,* Volume 2265.

Bak, C., Forsting, A. M. & Sorensen, N. N., 2020. The influence of leading edge roughness, rotor control and wind climate on the loss in energy production. *Journal of Physics: Conference Series,* 1618(5), p. 052050.

Bak, C. & Meyer Forsting, A., 2023. SALT - Simplified Aerodynamic Loss Tool (1.0.0 - beta). *DTU Wind, Technical University of Denmark.*

Campobasso, M. S. et al., 2025. *Validation of the Predictive Capabilities of Computational Aerodynamics codes to Assess Eroded Blade Performance: First Aerodynamic Benchmark,* s.l.: IEA Wind TCP.

Ehrmann, R. S. & White, E. B., 2015. *Effect of Blade Roughness on Transition and Wind Turbine Performance.,* s.l.: s.n.

Ehrmann, R. S. et al., 2013. *Realistic Leading-Edge Roughness Effects on Airfoil Performance.* s.l., AIAA.

Ehrmann, R. & White, E., 2014. *Influence of 2D Steps and Distributed Roughness on Transition on a NACA 63(3)-418.* s.l., AIAA.

Gaertner, E. et al., 2020. *Definition of the IEA 15-Megawatt Offshore Reference Wind Turbine,* s.l.: International Energy Agency (NREL/TP-75698).

Kelley, C. L., 2015. *Aerodynamic design of the National Rotor Testbed,* s.l.: Sandia National Laboratories.

Larsen, T. J. & Hansen, A. M., 2019. How 2 HAWC2, the user's manual. *DTU Wind,* Issue Risø-R-1597.

Maniaci, D. C., Westergaard, C., Hsieh, A. & Paquette, J. A., 2020. Uncertainty Quantification of Leading Edge Erosion Impacts on Wind Turbine Performance. *Journal of Physics: Conference Series,* 1618(Turbine Technology).

Maniaci, D. C., Westergaard, C., Hsieh, A. & Paquette, J. A., 2020. Uncertainty Quantification of Leading Edge Erosion Impacts on Wind Turbine Performance. *Journal of Physics: Conference Series,* 1618(5), p. 052082.

Maniaci, D. C. et al., 2016. Experimental Measurement and CFD Model Development of Thick Wind Turbine Airfoils with Leading Edge Erosion. *Journal of Physics: Conference Series,* 753(2).

Maniaci, D., Hsieh, A., deVelder, N. & Paquette, J., 2025. *Variation of Erosion Power Loss with Turbine Model.* Roskilde, Denmark, s.n.

Maniaci, D., MacDonald, H., Paquette, J. & Clarke, R., 2022. *Leading Edge Erosion Classification,* s.l.: IEA Wind TCP.

Meyer Forsting, A. R. et al., 2022. A spectral model generalising the surface perturbations from leading edge erosion and its application in CFD. *IOP Publishing.*

NREL, n.d. *OpenFAST.* [Online]
Available at: https://webserver.nrel.gov/wind/nwtc/openfast.html
[Accessed 28 02 2025].

Prieto, R. & Karlsson, T., 2021. A model to estimate the effect of variables causing erosion in wind turbine blades. *Wind Energyyy,* Volume 24, p. 1031–1044.

Sareen, A., Sapre, C. A. & Selig, M. S., 2014. Effects of leading edge erosion on wind turbine blade performance. *Wind Energy,* 17(10).

Visbech, J. et al., 2024. Aerodynamic effects of leading-edge erosion in wind farm flow modeling. *Wind Energy Science,* pp. 1811-1826.

Zahle, F. et al., 2024. *Definition of the IEA Wind 22-Megawatt Offshore Reference Wind Turbine,* s.l.: Technical University of Denmark.